



Contents lists available at SciVerse ScienceDirect



Applied Surface Science

journal homepage: www.elsevier.com/locate/apsusc

Corrosion inhibition behavior of propyl phosphonic acid–Zn²⁺ system for carbon steel in aqueous solution

M. Prabakaran^a, M. Venkatesh^b, S. Ramesh^{a,*}, V. Periasamy^a^a Department of Chemistry, The Gandhigram Rural Institute-Deemed University, Gandhigram, 624302, Tamilnadu, India^b Organic Chemistry Division, School of Advanced Sciences, VIT University, Vellore, 632014, India

ARTICLE INFO

Article history:

Received 2 February 2013

Received in revised form 18 March 2013

Accepted 20 March 2013

Available online xxx

Keywords:

Corrosion inhibition

Carbon steel

Propyl phosphonic acid

Gravimetric

Potentiodynamic

Impedance

ABSTRACT

The effectiveness of propyl phosphonic acid (PPA) as a corrosion inhibitor in association with a bivalent cation like Zn²⁺ has been studied. An eco-friendly inhibitor in controlling corrosion of carbon steel in neutral aqueous medium in the absence and presence of Zn²⁺ has been evaluated by gravimetric method. Impedance studies of the metal/solution interface indicated that the surface film is highly protective against the corrosion of carbon steel in the aqueous environment. Potentiodynamic polarization studies showed that the inhibitor is a mixed inhibitor. X-ray photoelectron spectroscopic analysis (XPS) of the protective film exhibited the presence of the elements viz., iron, phosphorus, oxygen, carbon and zinc. The chemical shifts in the binding energies of these elements inferred that the surface film is composed of oxides/hydroxides of iron(III), Zn(OH)₂ and [Fe(II)/(III)–Zn(II)–PPA] complex. Further, the surface analysis techniques viz., FT-IR, AFM and SEM studies confirm the formation of an adsorbed protective film on the carbon steel surface. Based on all these results, a plausible mechanism of corrosion inhibition is proposed.

© 2013 Elsevier B.V. All rights reserved.

1. Introduction

Carbon steel is the primary material used in the fabrication of cooling water systems and other industrial water distribution systems. In order to control corrosion of carbon steel in such systems, application of corrosion inhibitors is a widely used method [1]. Due to environmental restrictions imposed on heavy metal ion based corrosion inhibitors, the focus has been shifted to environmentally friendly corrosion inhibitors [2]. The inhibitors are extremely effective that even in very small concentrations they effectively reduce the corrosion rate. One of the main trends in inhibitor research is the study of corrosion inhibition and scale resistance properties of organic compounds. The use of organic phosphonic acids to protect carbon steel against corrosion has been the subject of various workers [3–6]. They have been widely used as water treatment agents because of their low toxicity, high stability and corrosion inhibition activity in neutral aqueous media [7,8]. Phosphonate based formulations are well known as corrosion inhibitors for carbon steel in aqueous environments. Synergistic effect existing between phosphonic acids and zinc ions on the inhibition of metals corrosion has already been studied by several researchers [9–12]. It is well known

that short-chain substituted phosphonic acids are good corrosion inhibitors for iron and low alloyed steels [13,14].

In the present work, the inhibitive effect with a new organic inhibitor viz., propyl phosphonic acid (PPA) and Zn²⁺ ions in controlling the corrosion of carbon steel in neutral aqueous environment containing low chloride has been studied by the gravimetric studies. The corrosion inhibition was further investigated by means of polarization curves and electrochemical impedance spectroscopy (EIS). Surface analytical techniques, viz., X-ray photoelectron spectroscopy (XPS), Fourier transform infrared spectroscopy (FT-IR), atomic force microscopy (AFM) and scanning electron microscopy (SEM) were used to investigate the nature of protective film formed on the metal surface. A plausible mechanism of inhibition of corrosion is proposed. For all these studies, aqueous solution of 60 ppm chloride has been chosen as control because of the water used in cooling water systems is generally either demineralized water or unpolluted surface water.

2. Experimental

2.1. Material

Propyl phosphonic acid (PPA) obtained from Alderich Chemical Company Inc., USA, was used as such in the present study. The molecular structure of the PPA is shown in Fig. 1. Zinc sulphate (ZnSO₄·7H₂O), sodium chloride and other reagents were analytical

* Corresponding author. Tel.: +91 0451 2452371; fax: +91 0451 2454466.

E-mail addresses: drsramesh.56@yahoo.com, prabakar05@gmail.com (S. Ramesh).

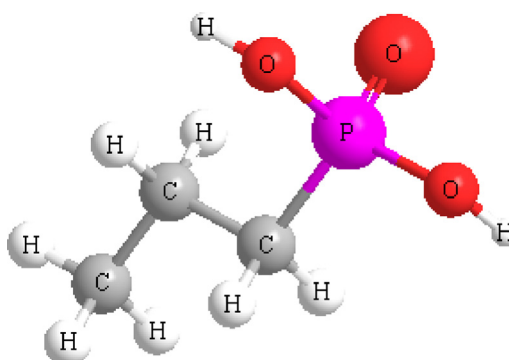


Fig. 1. Molecular structure of propyl phosphonic acid (PPA).

grade chemicals. All the solutions were prepared using triple distilled non-deaerated water.

2.2. Preparation of specimens

Carbon steel specimens (0.02–0.03% S, 0.03–0.08% P, 0.4–0.5% Mn, 0.1–0.2% C and the rest iron) of dimensions 3.5 cm × 1.5 cm × 0.2 cm, were polished to a mirror finish with 1/0, 2/0, 3/0, 4/0, 5/0, and 6/0 emery polishing papers respectively, degreased with acetone, dried and used for gravimetric measurements, FT-IR, AFM and SEM for surface studies. The dimensions of the specimens with 1.0 cm × 1.0 cm × 0.1 cm was used for XPS analysis.

2.3. Gravimetric measurements

In all gravimetric experiments, the polished specimens were weighed and immersed in duplicate, in 100 mL control solution in the absence and presence of inhibitor formulations of different concentrations, for a period of 7 days and pH 7.0 was maintained for all test solutions. Then, the specimens were reweighed after washing and drying. The weights of the specimens before and after immersion were determined with mettler electronic balance AE 240 model with a readability of 0.1 mg. Corrosion rates of carbon steel in the absence and presence of various inhibitor formulations are expressed in mdd. Inhibition efficiencies (IE) of the inhibitor were calculated by using the formula:

$$IE_g(\%) = \left[\frac{CR_0 - CR_1}{CR_0} \right] \times 100 \quad (1)$$

where CR_0 is the corrosion rate in the absence of inhibitor and CR_1 is the corrosion rate in the presence of inhibitor

2.4. Atomic absorption spectroscopy

Analysis of Zn^{2+} present in the test solution after immersion of carbon steel in inhibitor containing Zn^{2+} ions and phosphonate for seven days was carried out using PerkinElmer Atomic Absorption Spectrophotometer, model AAnalyst 100.

2.5. Electrochemical studies

Both the polarization and electrochemical impedance spectroscopic (EIS) studies were carried out using Electrochemical analyzer model CHI 160D provided with a rectangular specimen of carbon steel as working electrode, platinum foil as the counter electrode and saturated calomel electrode as reference electrode. The reference electrode was placed close to the working electrode to minimize IR contribution. The three electrode set up was immersed in control solution of volume 100 mL both in the absence

and presence of various inhibitor formulations and allowed to attain a stable open circuit potential (OCP).

The polarization studies were made in the potential range of ±200 mV from the open circuit potential at a sweep rate of 1 mV/s. the corrosion potential (E_{corr}), corrosion current (I_{corr}) and anodic Tafel slope (b_a) and cathodic Tafel slope (b_c) were obtained by extrapolation of anodic and cathodic regions of the Tafel plots. The values of inhibition efficiencies (IE_p) were calculated from I_{corr} values using the equation,

$$IE_p(\%) = \left[\frac{I_{corr} - I'_{corr}}{I_{corr}} \right] \times 100 \quad (2)$$

where I_{corr} and I'_{corr} are the corrosion current densities in case of control and inhibited solutions, respectively.

Electrochemical impedance spectra in the form of Nyquist plots and Bode plots were recorded at OCP in the frequency range from 60 kHz to 10 mHz. The impedance parameters viz., charge transfer resistance (R_{ct}) and constant phase element (CPE) were obtained from the Nyquist plots. The inhibition efficiencies (IE_i) were calculated using the equation,

$$IE_i(\%) = \left[\frac{R'_{ct} - R_{ct}}{R'_{ct}} \right] \times 100 \quad (3)$$

where R_{ct} and R'_{ct} are the charge transfer resistance values in the absence and presence of the inhibitor.

2.6. Surface examination studies

The carbon steels were immersed in various test solutions for a period of seven days. Then, they were taken out and dried. The nature of the film formed on the surface of the metal specimen was analyzed by XPS, FTIR, AFM and SEM.

2.6.1. X-ray photoelectron spectroscopy

XPS measurements of the protective films were carried out with a Kratos analytical photoelectron spectrometer model AXIS 165 with monochromated Al K α X-ray source (1486.6 eV) operated at 100 W and with a resolution of 0.1 eV. Both the survey spectra and deconvolution spectra were recorded at four spots on each specimen. The average of the four measurements is reported. The spectra were collected at an electron take-off angle of 90°. Analyzer pass energy was 80 eV, with a step of 0.1 eV for the elements of interest, namely Fe 2p, P 2p, C 1s, O 1s, Zn 2p and Cl 2p. Binding energies for the deconvolution spectra were corrected individually for each measurement set, based on a value of 285.0 eV for the C–C component of C 1s.

2.6.2. FT-IR studies

FTIR spectra of pure PPA and the surface film were recorded using KBr pellet method using JASCO 460 PLUS Spectrophotometer in the wave number range of 4000–400 cm^{-1} with a resolution of 4 cm^{-1} .

2.6.3. Atomic force microscopy

Atomic force microscope was used for surface morphology studies. The protective films were examined with atomic force microscope (AFM) Nano Surf Easy Scan-2. The topography of the entire samples for a scanned area of 5 $\mu\text{m} \times 5 \mu\text{m}$ (25 μm^2) is evaluated for a set point of 20 nN and a scan speed of 10 mm/s. The three and two-dimensional topography of surface films gave various roughness parameters of the film.

2.6.4. Scanning electron microscopy

The polished carbon steel specimens were immersed in 60 ppm chloride solutions in the absence and in the presence of the inhibitor. After 7 days, the specimens were taken out, washed with

Table 1

Inhibition efficiencies (%) obtained by gravimetric studies of carbon steel in absence and presence of inhibitor (PPA-Zn²⁺).

PPA (ppm)	Zn ²⁺ (ppm)							
	0	10	20	50	75	100	125	150
0	—	17	25	2	6	3	2	11
10	12	24	30	4	9	5	5	13
20	17	21	31	7	10	36	22	23
50	14	27	35	28	39	45	42	56
75	12	26	30	45	70	90	70	67
100	10	12	26	35	77	66	76	82
125	4	20	30	32	73	57	85	87
150	3	17	33	20	18	55	72	84

distilled water and dried. The SEM photographs of the surfaces of the specimens were obtained using HITACHI S-3000H model with a resolution of 3.5 nm.

3. Results and discussion

3.1. Evaluation of corrosion inhibition

3.1.1. Gravimetric studies

The results of corrosion rate and inhibition efficiency (IE %), obtained from gravimetric method at different concentrations of inhibitor for the corrosion of carbon steel immersed in an aqueous solution containing 60 ppm Cl⁻, in the absence and presence of Zn²⁺, are given in Table 1. Fig. 2 shows the inhibition efficiency as a function of concentration of PPA. It is evident that PPA by itself is a poor corrosion inhibitor. Also, zinc ions are found to be corrosive. However, interestingly PPA-Zn²⁺ ions combination offers good corrosion inhibition at 75 ppm of PPA and 100 ppm of Zn²⁺ ions. At low concentrations of 10, 20 and 50 ppm of Zn²⁺ ions along with PPA (10–150 ppm), only moderate inhibition efficiencies were observed. When the concentration of Zn²⁺ ions and PPA were raised to 80 ppm of Zn²⁺ ions and 75 ppm of PPA, respectively an inhibition efficiency of 70% was observed. But, with increasing concentration of Zn²⁺ ions, keeping PPA constant at 75 ppm, the maximum inhibition efficiency was achieved. This may be explained as follows. At lower concentrations of Zn²⁺ ions, the PPA is precipitated as PPA-Zn²⁺ complex in the bulk of the solution. PPA is not transported towards the metal surface. Only on increasing concentrations of

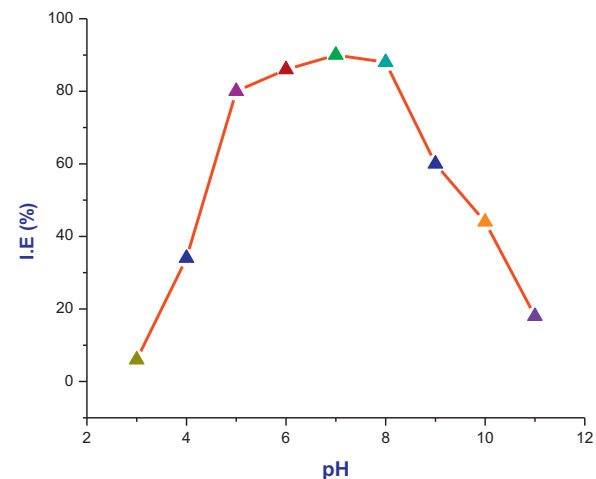


Fig. 3. Effect of pH.

Zn²⁺ ions, the maximum inhibition efficiencies are obtained. A synergistic effect is noticed between PPA and Zn²⁺ ions. When 100 ppm of Zn²⁺ ions are added to PPA, PPA-Zn²⁺ complex is in solubilized form. It diffuses from bulk of the solution to metal surface. The [Fe(III)/Fe(II)-PPA-Zn²⁺] complex is formed. A thin multicolored film is observed on the surface of the inhibited metal during the gravimetric studies. The maximum inhibition efficiency obtained from the above formulation is 90%. It can be interpreted that at lower concentrations of Zn²⁺ ions, the Zn²⁺ ions were insufficient to form a protective film with PPA on the metal surface.

3.1.2. Effect of pH

The influence of pH on corrosion rate of carbon steel in the presence of inhibitor system and the maximum inhibition efficiency obtained in the gravimetric measurements were studied. The effect of pH for the synergistic formulation consisting of PPA (75 ppm) + Zn²⁺ (100 ppm), in the pH range of 3–11 is shown Fig. 3. The highest inhibition efficiency could be obtained in the pH range 6–8. But, when the pH is decreased from 6 to 3, the inhibition efficiency is reduced to 6% and on increasing pH range from 8 to 11, the inhibition efficiency is reduced to 18%. The reasons for decrease in inhibition efficiency in more alkaline and acidic environments are explained under the mechanistic aspects.

3.2. Atomic absorption spectroscopy

The solution containing 60 ppm chloride, 75 ppm PPA and 100 ppm Zn²⁺ ions in which carbon steel specimens were immersed for 7 days was analyzed for Zn²⁺ ions by AAS. The results show that out of 0.1529 mmol of Zn²⁺ ions, 0.1445 mmol of Zn²⁺ ions have diffused from the bulk of the solution to the metal surface. The results are provided in Table 2. It can be interpreted that the appreciable amount of Zn²⁺ ions have diffused from the bulk of the solution to the metal surface and incorporated in the protective film.

Table 2

Analysis of solution for zinc ions.

[Zn ²⁺] present in solution (100 mL) before immersion of metal specimen	[Zn ²⁺] present in solution (100 mL) after immersion of metal specimen for 7 days (mmol)	[Zn ²⁺] diffused from bulk of the solution to metal specimen (mmol)
0.1529	0.0084	0.1445

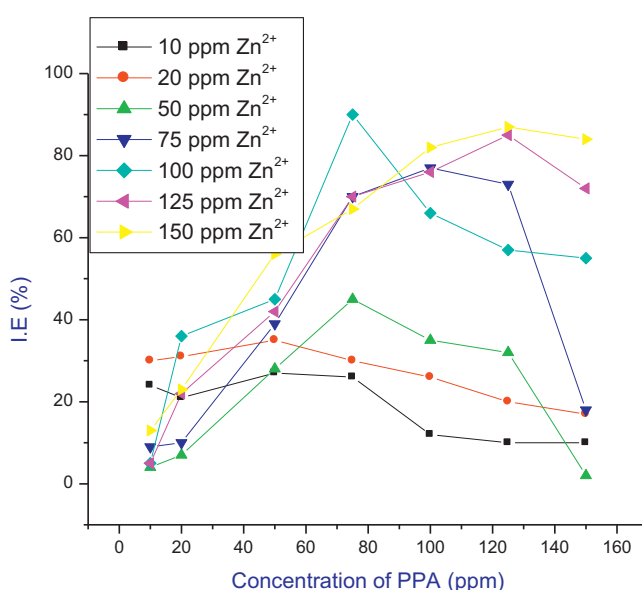


Fig. 2. Inhibition efficiency as a function of concentration of PPA.

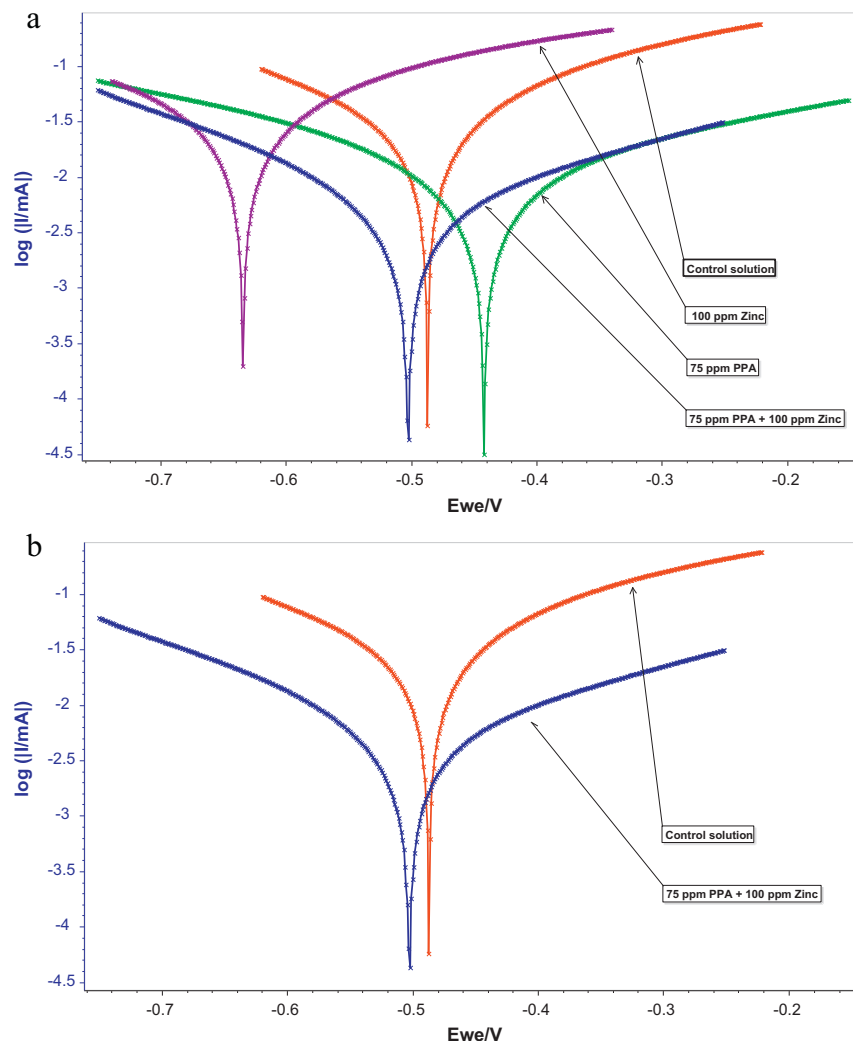


Fig. 4. (a) Potentiodynamic polarization curves of carbon steel immersed in various test solutions. (b) Potentiodynamic polarization curves of carbon steel immersed in control solution and inhibitor solution.

3.3. Potentiodynamic polarization studies

The potentiodynamic polarization curves of carbon steel electrode in control solution containing 60 ppm chloride solution at pH 7 in the absence and presence of various inhibitor combinations are shown in Fig. 4a. Various Tafel parameters, i.e., corrosion potential (E_{corr}), corrosion current density (I_{corr}), anodic Tafel slope (β_a), cathodic Tafel slope (β_c) and the inhibition efficiencies ($I.E_p$) are listed in Table 3. An examination of Table 3 shows that the corrosion potential (E_{corr}) in case of the control is -487.62 mV/SCE and the corresponding corrosion current density (I_{corr}) is $22.68 \mu A/cm^2$. When of PPA alone was added to the control, the corrosion potential is shifted to a more anodic side and its corrosion current

density is reduced to $8.02 \mu A/cm^2$. The anodic Tafel (β_a) slope for PPA has been shifted more anodically (118 mV/decade) than the cathodic Tafel (β_c) slope (62 mV/decade). In the literature, it was reported that phosphonates in general are anodic inhibitors [9]. When 100 ppm of Zn^{2+} is added to the control, the corrosion potential is shifted to the cathodic side and the shift in cathodic Tafel slope is greater. Contrary to the result obtained in the case of PPA, Zn^{2+} increased the rate of corrosion as implied by increase in corrosion current density. In the presence of Zn^{2+} , the increase in corrosion current density leads to increase in corrosion rate [15]. From the polarization curves shown in Fig. 4b, it is clear that for the combination of 75 ppm PPA and 100 ppm Zn^{2+} , the corrosion potential is shifted to -501.92 mV/SCE and its corrosion current

Table 3

Corrosion parameters of carbon steel immersed in the absence and in the presence of inhibitor obtained by potentiodynamic polarization studies.

Concentration (ppm)		Tafel parameters				
PPA	Zn^{2+}	E_{corr} (mV/SCE)	I_{corr} ($\mu A/cm^2$)	β_a (mV/decade)	β_c (mV/decade)	$I.E_p$ (%)
–	–	-487.62	22.68	209	212	–
75	–	-441.99	8.02	327	274	65
–	100	-633.83	23.30	208	209	–
75	100	-501.92	4.29	198	276	81

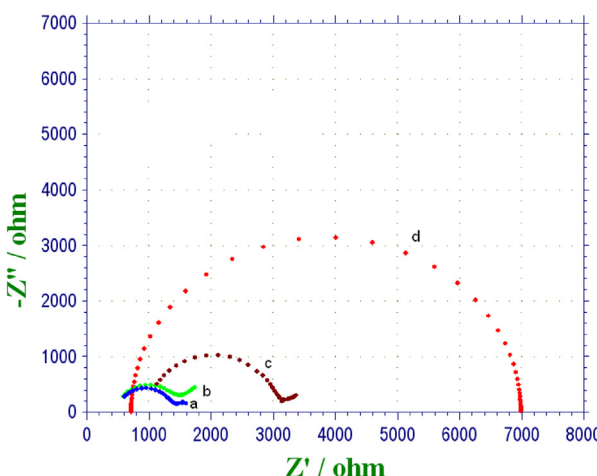


Fig. 5. Nyquist plots of carbon steel immersed in various test solutions. (a) 60 ppm Cl^- ions; (b) 60 ppm Cl^- ions + 100 ppm Zn^{2+} ions; (c) 60 ppm Cl^- ions + 75 ppm PPA; (d) 60 ppm Cl^- ions + 75 ppm PPA + 100 ppm Zn^{2+} ions.

density is also reduced when compared to the control. Thus, it is evident that this formulation acts as an effective mixed type inhibitor. There is a slight shift in corrosion potential to a more cathodic side and the shift in cathodic Tafel slope (64 mV/decade) is greater than the shift in anodic Tafel slope shift (11 mV/decade). The corrosion current is significantly decreased from $22.68 \mu\text{A}/\text{cm}^2$ to $4.29 \mu\text{A}/\text{cm}^2$, corresponding to an inhibition efficiency of 81%. Thus, the synergistic mixture of 75 ppm PPA and 100 ppm Zn^{2+} is proved to be an effective corrosion inhibitor for carbon steel. These results indicate that the binary inhibitor formulation retards both the anodic dissolution of carbon steel and oxygen reduction at cathodic sites in the corrosion inhibition process. Similar phosphonate-based formulations were reported to be mixed inhibitors [16]. A significant observation related to the inhibition efficiency values is to be noted. If the inhibition efficiency values obtained from gravimetric (IE_g), polarization (IE_p), and EIS (IE_i) studies are compared, slight differences are observed. It is suggested that the inhibition efficiency values obtained from various methods may not be strictly comparable when the immersion times used in these methods are not the same [17].

3.4. Electrochemical impedance studies

Nyquist plots for carbon steel immersed in 60 ppm of Cl^- solution at pH 7 in the absence and presence of various formulations are shown in Fig. 5 (Bode plots are not shown). The impedance parameters calculated from the Nyquist plots are given in Table 4. The impedance diagrams obtained are not perfect semicircles and this difference has been attributed to frequency dispersion as a result of roughness in homogenates of the electrode surface [18]. The charge transfer resistance (R_{ct}) values are calculated from the difference in impedance at lower and higher frequencies, as suggested by Tsuru et al. [19]. To obtain the double layer capacitance (C_{dl}), the frequency at which the imaginary component of the impedance maximum, ($-Z_{max}''$), is found and C_{dl} values are obtained from the equation:

$$f(-Z_{max}'') = \frac{1}{2\pi C_{dl} R_{ct}} \quad (4)$$

The inhibition efficiency of the inhibitor on the corrosion of steel is calculated by charge transfer resistance given in Eq. (3).

The experimental data obtained from Nyquist plots are fitted by the equivalent electrical circuit shown in Fig. 6. Such an equivalent circuit was also discussed by several researchers who obtained

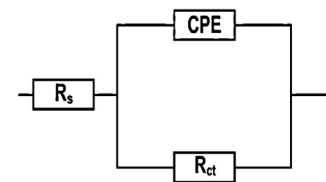


Fig. 6. Nyquist plots are fitted by the equivalent electrical circuit.

similar depressed semicircles with single time constant [20–22]. In this case, the constant phase element, CPE is introduced in the circuit instead of a pure double layer capacitor to give a more accurate fit [23]. The impedance function of a CPE is described by the equation:

$$Z_{CPE} = Y^{-1}(j\omega)^{-n} \quad (5)$$

where R_s is solution resistance, R_{ct} is the charge transfer resistance and CPE is a constant phase element, Y is the magnitude of the CPE, ω is the angular frequency ($2\pi f_{max}$) and the deviation parameter n is a valuable indicator of the nature of the metal surface and reflects microscopic fluctuations of the surface. For $n=0$, Z_{CPE} represents a resistance with $R=Y^{-1}$; for $n=-1$ an inductance with $L=Y^{-1}$, for $n=1$ an ideal capacitor with $C=Y$ [24]. The value range of n for a real electrode is often between 0 and 1. The smaller value of n is rougher electrode surface and more serious corrosion of electrode [25].

In the present study, a small semicircle with an R_{ct} value of 943Ω is observed for the control alone. A similar semicircle is also obtained when 100 ppm of Zn^{2+} is added to the control. Due to Zn^{2+} ions, R_{ct} is increased and CPE value is decreased with a slight increase in the value of n . By the addition of 75 ppm of PPA to the control, a single and slightly depressed semicircle with high R_{ct} value is obtained. The capacitance value is decreased and n value is increased. These observations can be attributed to the presence of organic inhibitor molecules in the double layer and control of the corrosion processes to some extent. When, the combination of 75 ppm of PPA and 100 ppm of Zn^{2+} is considered in the presence of the control, a large depressed semicircle is observed from high frequency to low frequency regions in the Nyquist plot, indicating that the charge transfer resistance becomes dominant in the corrosion processes due to the presence of a protective film on the metal surface. This result is supported by the significant decrease in CPE and an increase in n value. The semicircle obtained in the presence of PPA/ Zn^{2+} represents an R_{ct} value of 6271Ω , which is greater than that observed in case of the control. The CPE value at the metal/solution interface is found to decrease from $578 \mu\text{F cm}^{-2}$ in the case of the control to $452 \mu\text{F cm}^{-2}$ in the case of the binary inhibitor formulation. This is because of the replacement of water molecules in the electrical double layer by the organic molecules having low dielectric constants [26].

The value of n is considerably increased to 0.86 in the presence of the binary inhibitor system, suggesting a decrease of inhomogeneity of the interface during inhibition process. These results indicated that there is formation of a non-porous and protective film in the presence of the binary inhibitor formulation. The inhibition efficiency obtained from impedance studies is found to be 85%. Several authors who studied the inhibitory effects of phosphonate-based corrosion inhibitors have also reported that there is formation of a thick and less permeable protective film on the metal surface [9,16]. They also concluded that the protective film consists of phosphonate–metal complexes. The results also imply the synergistic action operating between PPA and Zn^{2+} . This is in agreement with the inferences drawn from gravimetric studies and polarization studies.

Table 4

A.C. impedance parameters of carbon steel immersed in the presence and absence of inhibitor obtained by A.C. impedance spectra.

Concentration (ppm)		Charge transfer resistance R_{ct} (Ω)	Constant phase element CPE ($\mu\text{F}/\text{cm}^2$)	Constant exponent n	I.E. (%)
PPA	Zn ²⁺				
0	0	943	578	0.60	–
100	0	1067	489	0.68	11
0	75	2266	379	0.74	58
75	100	6271	452	0.86	85

3.5. Surface examination studies

3.5.1. X-ray photoelectron spectroscopy

XPS patterns of the protective films formed on the carbon steel surface immersed in aqueous environment of 60 ppm chloride at neutral pH in the absence and the presence of the inhibitor were recorded. The XPS were interpreted with the help of the literature data for various elements exhibiting peaks at characteristic binding energy levels. The XPS deconvoluted spectra of the individual elements for the above system (control) relating to chlorine, carbon, oxygen and iron are not shown in Figures. The peaks at 287.5 eV and 290.4 eV correspond to C 1s which appeared even in the absence of any inhibitor. These carbon peaks are due to residual carbon from oil vapours of the diffusion pump while recording the XPS spectrum with the instrument. Similar carbon peaks are reported in the literature in XPS spectrum for the same reason. These peaks appeared due to surface contamination [27–30].

The presence of adsorbed water molecules is reported to exhibit the peak at 533.2 eV [31,32]. However, there is formation of a brown film consisting of oxides/hydroxides of iron on carbon steel surface. Therefore, the broad peak due to O 1s at 533.4 eV in the present study also, can be interpreted to occur due to the presence of iron only, adsorbed H₂O molecules and also oxides/hydroxides of iron. This interpretation can be seen along with the interpretation of iron peak discussed below. In the Fe 2p deconvoluted spectrum in case of the control, two peaks appear for iron, one at 713.9 eV and that at 727.1 eV. The former peak corresponds to Fe 2p_{3/2} and the latter peak corresponds to Fe 2p_{1/2}. The shifts in both the peaks from the corresponding binding energy values of elemental iron are quite significant. The peak due to Fe 2p_{3/2} is interpreted for the determination of chemical state of iron in the surface film. The peak of Fe 2p_{3/2} at 713.9 eV is the one shifted from 707.0 eV, the characteristic elemental binding energy of Fe 2p_{3/2} [33]. Such a large shift of 6.9 eV, suggest that iron is present in Fe³⁺ state in the surface film. The peak at 713.9 eV can also be ascribed to the presence of γ-Fe₂O₃, Fe₃O₄ and FeOOH [16,34–36]. The peak at 727.1 eV corresponds to Fe 2p_{1/2} which also indicates the presence of iron oxides. The chlorine 2p_{1/2} peak at 201.11 eV indicates the presence of lower amount of chlorine in the surface film. The XPS pattern of the surface film of carbon steel immersed in 60 ppm chloride ions, 75 ppm PPA and 100 ppm Zn²⁺ ions for a period of 7 days is given in Fig. 7. The

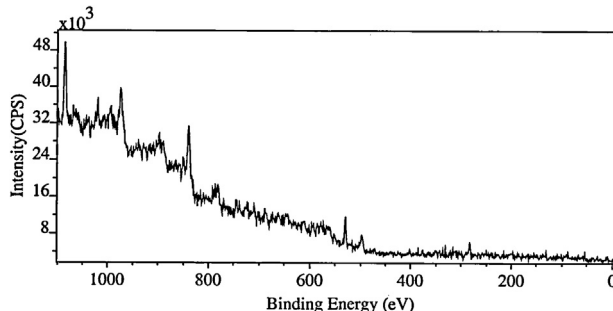


Fig. 7. XPS spectrum of the general survey of the inhibited surface film (60 ppm Cl⁻ ions + 75 ppm PPA + 100 ppm Zn²⁺ ions).

XPS deconvoluted spectra of the individual elements of phosphorous, carbon, oxygen, zinc, iron and chlorine are given in Fig. 8a–f. Two peaks of P 2p_{3/2} are observed, one at 132.9 eV and 134.1 eV (Fig. 8a). The shifts in the binding energy are noticed from 130 eV for the P 2p_{3/2} and 131 eV for P 2p_{1/2} elemental binding energy of phosphorous compounds and iron [14,37,38]. Labjar et al. [39] had studied ATMP treated carbon steel surface by XPS spectra of P 2p and concluded that a binding energy of 133.5 eV and 132.8 eV were attributable to the phosphonates, the other peak was mainly attributed to CH₂P(O)(OH)₂ [40–42]. Kar and Singh have reported that the phosphorous showed two peaks one at 139.1 eV and other at 130.1 eV and identified that the shifts were due to presence of phosphonate in NTP which leads to the formation of protective film on the metal surface [43].

The binding energy of the FePO₄ has been reported in the range between 133.3 and 133.8 eV. The binding energies for phosphonates in the surface film for iron or steel immersed in solution containing phosphonates, ortho phosphonates or poly phosphates are also reported to be in the range between 132.9 and 133.8 eV [37,38]. Therefore, the shift in the peak observed in the present study is attributable to Fe-phosphonate complex. The C 1s spectrum has 3 peaks, one is the more intense peak at 284.7 eV and other two are less intense peaks at 285.7 and 287.75 (Fig. 8b). The presence of multiple peaks in the C 1s spectrum in the case of the inhibitor can be attributed to various carbon environments present in PPA. The intensity of the C 1s peaks in the presence of the inhibitor is about twice as that of the peak in the case of control. This interpretation can be supported from studies reported in the literature [20,28,29,37].

In the O 1s spectrum, the peaks were observed at 530.6 eV and 531.8 eV (Fig. 8c). The O 1s peak observed at 530.6 eV is due to O²⁻, the presence of O²⁻ in the surface film may be in the form of oxides and hydroxides of Fe(III) [16,29,44]. The O 1s peak of high intensity was observed at 531.8 eV. It may be interpreted as follows. The XPS of the surface film shows the presence of carbon, phosphorous, iron and zinc. It means that PPA is present on the surface, zinc is present as Zn²⁺ and the interpretation given in the case of Fe 2p indicates the presence of Fe₂O₃, Fe₃O₄ and FeOOH. Hence, the O 1s peak observed in the inhibited surface films can be ascribed to the presence of Zn(OH)₂, Fe₂O₃, Fe₃O₄, FeOOH and/or Fe(OH)₂ and oxygen of PPA in the inhibited film [14,16,28,45]. The disappearance of the peak at 533.4 eV (from control solution) in the case of the inhibitor formulation indicates the absence of water molecules in the surface film, as they have been replaced by the inhibitor molecules. When the intensities of uninhibited (control solution) and inhibited one are compared, the intensities found in the case of inhibited surface film is more intense than in the case of control. This means that the water molecules have been replaced by the inhibitor molecules.

The binding energy of Zn 2p_{3/2} is shifted from 1021.4 eV for elemental zinc to 1022.4 eV and binding energy of Zn 2p_{1/2} is shifted from 1044 eV to 1045.3 (Fig. 8d). The Zn 2p_{3/2} peak is normally interpreted and ascribed to the presence of Zn(OH)₂ in the inhibited surface film and also to the involvement of Zn²⁺ in the complex formation with PPA [28,46]. XPS deconvoluted spectrum of iron is shown Fig. 8e. The Fe 2p_{3/2} peaks at 711.6 eV and 713.9 eV have shifted from 707 eV for elemental iron. Similar shifts were also

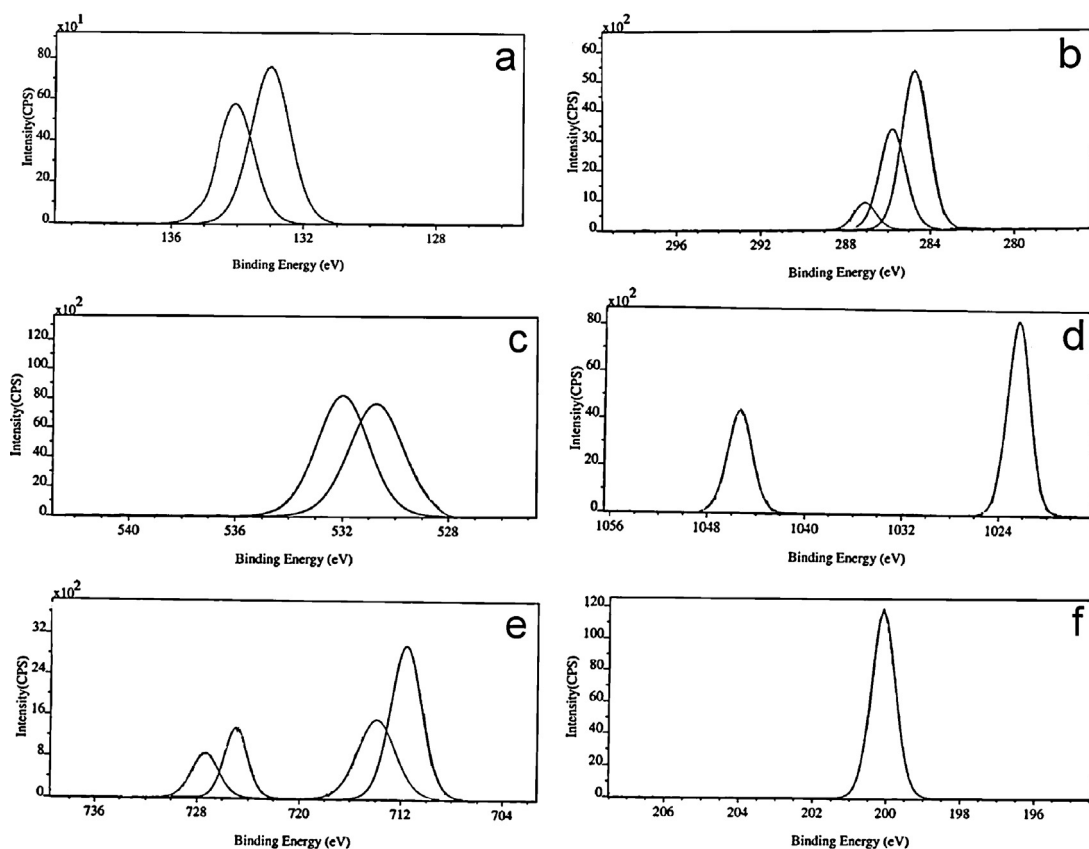


Fig. 8. XPS deconvolution spectra of (a) P 2p (b) C 1s (c) O 1s (d) Zn 2p (e) Fe 2p (f) Cl 2p.

observed by Felhosi et al. and Karman et al. [31,32]. The Fe 2p_{1/2} peaks which have also shifted from 720 eV to 725 eV. The peaks are not due to Fe²⁺, Fe³⁺ oxides and hydroxides but also due to Fe²⁺/Fe³⁺ in complexation with PPA (inhibitor molecule). The absence of any iron peak in this region in the present study also supports that iron does not exist in the Fe²⁺ state. Paszternak et al., reported that the Fe 2p_{3/2} and Fe 2p_{1/2} peaks were decomposed into two main compounds; the metallic iron (Fe 2p_{3/2} at 707 eV and Fe 2p_{1/2} at 719.5 eV) and the mixture of Fe³⁺ and Fe²⁺ (Fe 2p_{3/2} at 711 eV and Fe 2p_{1/2} at 724 eV) and confirmed the dominant chemical state in the oxide is the Fe³⁺ in their alkyl phosphonated film on iron surface [47].

Along with the elements discussed above, the deconvoluted XPS spectrum in the case of chlorine in inhibited surface is shown in Fig. 8f. A peak at 200.1 eV appeared for chlorine where as in the case of control, a low intensity chlorine peak is seen at 201 eV. Labjar et al. have pointed out that a peak which appears at 713.8 eV is attributed to the presence of a small amount of FeCl₃ on the metal surface [39]. Moreover, Rossi and co-workers have suggested that chlorine has been repelled by PO₃³⁻ away from the metal surface [48]. This indicates the decreased adsorption of chlorine leading to higher resistance against localized corrosion. The present study also shows that the presence of smaller amounts of chlorine and subsequent adsorption of aggressive ions on metal surface is decreased thereby allowing inhibitor molecules to cover the entire surface and protecting the metal. The results of the XPS clearly revealed the shifts in binding energies for the elements P, C, O, Fe and Zn. It is suggested that there is formation of an insoluble complex by the inhibitor molecules. Fang et al., confirmed the presence of a complex between Fe(II) and ATMP on the metal surface from XPS analysis. Thus, the protective surface film consists of mainly

[Zn(II)-PPA] complex, Zn(OH)₂, and small amounts of oxides and hydroxides of iron. The complex formed may be chemisorbed on the metal surface and got attached to the Fe(III) ions predominantly [17]. From XPS, it is seen that the protective film is formed upon the iron oxide film/layer, which is built upon iron metal. The inhibitor molecules are seen to be distributed throughout the oxide layers. From P 2p, it is clearly seen that the PPA is present in the protective film.

3.5.2. FT-IR studies

The FT-IR spectrum of pure Propyl phosphonic acid is shown in Fig. 9a. The stretching frequency made of P=O band in the region 1380–1140 cm⁻¹ and another band in the region 970–1188 cm⁻¹.

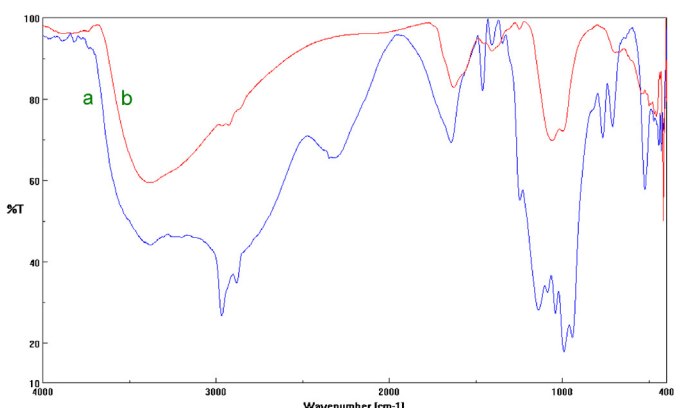


Fig. 9. FTIR Spectra of (a) pure PPA, (b) surface film.

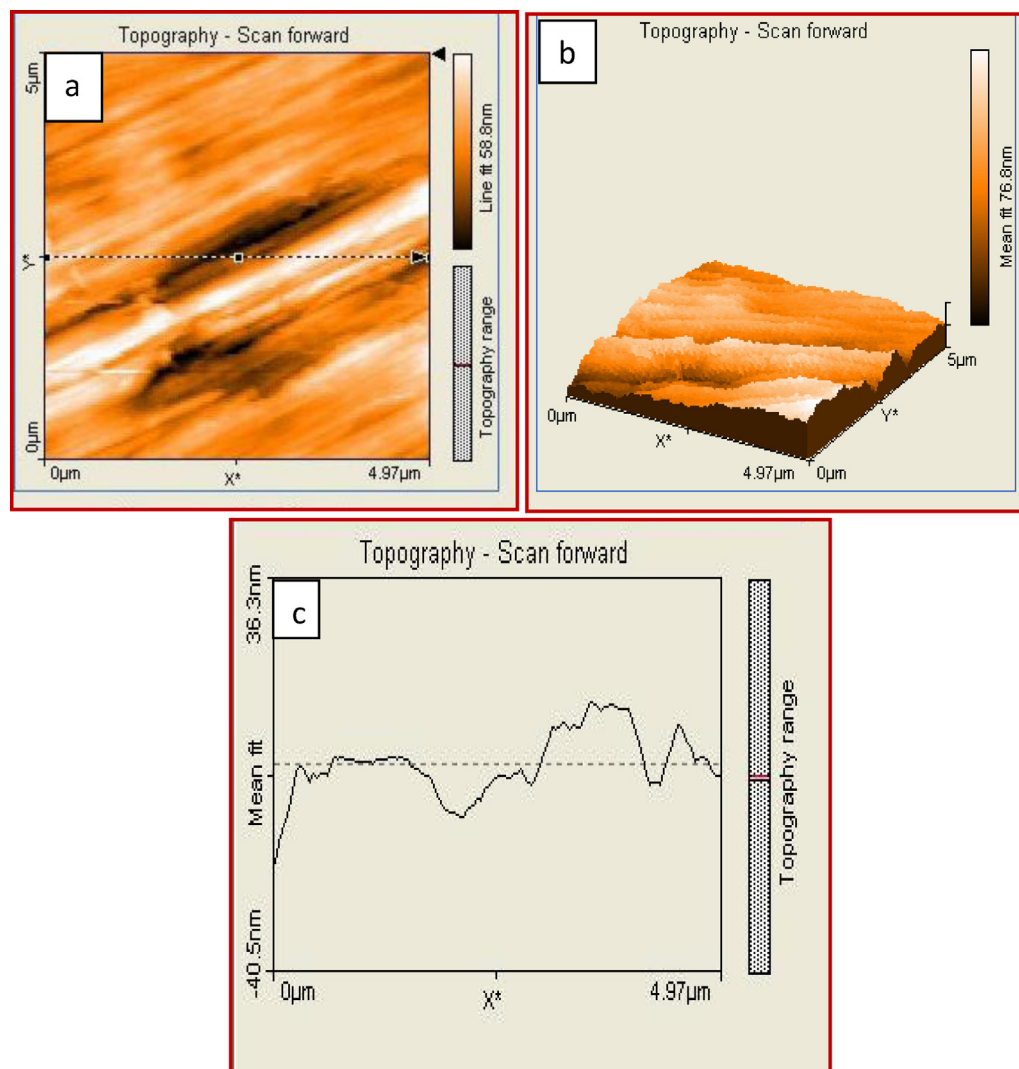


Fig. 10. AFM images and cross section analysis of polished metal surface.

The peak at 1139.72 cm^{-1} was assigned to P=O group while the peak at 993.16 was assigned to P-OH group [49,50]. The FTIR spectrum of 60 ppm Cl⁻, 75 ppm PPA and 100 ppm Zn²⁺ ions (surface film) is shown in Fig. 9b. In this case the inhibited surface film formed by the peak due to P=O is shifted from 1139.72 cm^{-1} to 1058.73 cm^{-1} . The P-OH stretching located at 993.16 cm^{-1} has disappeared. These results can be interpreted in terms of interaction between P⁺-O⁻ present in the phosphonate with metallic species, viz., Zn(II) and iron to form P-O-Zn and P-O-Fe bonds. This interpretation was also given by several authors, who worked on corrosion inhibition of carbon steel by phosphonates [9,10,51]. This also suggests that phosphonates are coordinated with metal ions resulting in the formation of [metal-phosphonate] complexes on the surface. The peak at 1407.78 cm^{-1} indicates the presence of Zn(OH)₂ on the metal surface film [12]. The broad band of the OH stretching and bending mode of water or hydroxides within the protective film appeared at 3405.67 cm^{-1} . There are many weak bands in the region between $1200\text{--}400\text{ cm}^{-1}$ and a peak of high intensity appeared at 433.91 cm^{-1} implying the presence of ferric and ferrous oxides and hydroxide in the protective film [52,53]. The FTIR spectra suggests that what the protective film may consist of [Fe(II)/Zn(II)-PPA], Zn(OH)₂ and small amounts oxides and hydroxides of iron.

3.5.3. Atomic force micrographs

Table 5 shows various AFM parameters obtained for the carbon steel surface immersed in different environments. Fig. 10 shows one and 3D AFM images of polished metal surface. Rms value 12 nm and ΔZ value 7.15 nm when compared with other thin film coated surface values indicate the absence of iron oxides on the smooth surface. Fig. 11 shows one and 3-D images of polished metal surface immersed in 60 ppm Cl⁻ ion solution indicating the formation of iron oxides by the increased Rms value 95 nm and ΔZ value of 579.2 nm. Fig. 12 shows one and 3-D images of carbon steel

Table 5

AFM parameters in different environments.

Environment	Period of immersion	AFM parameters	
		Rms value (nm)	ΔZ value (nm)
Polished metal	–	12	7.15
Polished metal + 60 ppm Cl ⁻	7 days	95	579.2
Polished metal + 60 ppm Cl ⁻ + 75 ppm PPA + 100 ppm Zn ²⁺	7 days	52	152.5

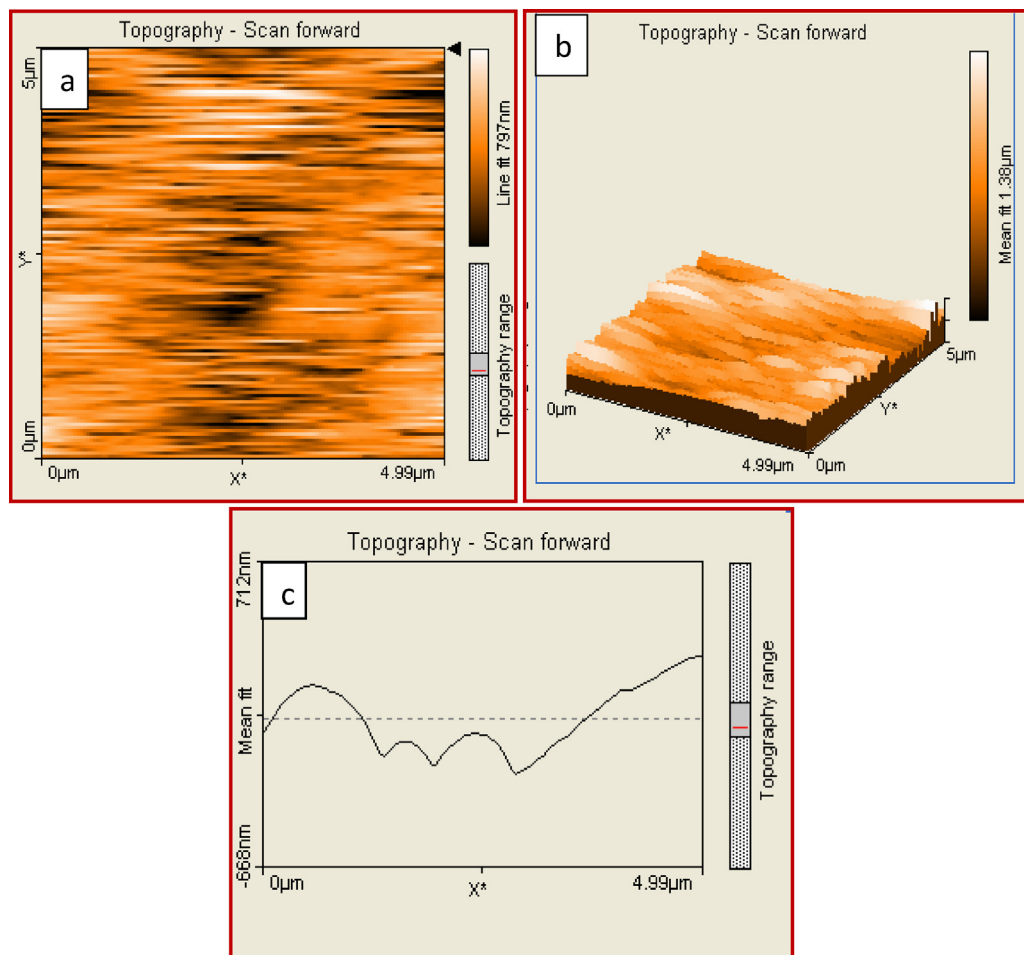


Fig. 11. AFM images and cross section analysis of polished metal surface immersed in control solution.

immersed in 60 ppm Cl^- + 75 ppm PPA + 100 ppm Zn^{2+} ions solution in which increased Rms value 52 nm and ΔZ value 152.5 representing the formation of protective thin film on the metal surface. These increased values strongly imply the formation of an inhibitive film by the addition of Zn^{2+} along with the phosphonic acid inhibitor system on the metal surface. These results are confirmed by the clearly visible differences among the typical cross section analysis profile of the samples. Similar reports have been observed in the literature [16,54,55].

3.5.4. Scanning electron microscopy

The SEM images of carbon steel containing 60 ppm Cl^- ions are shown in Fig. 13a. A SEM backscatter image of a carbon steel sample that had been exposed to an environment containing 60 ppm Cl^- ions, 75 ppm PPA and 100 ppm Zn^{2+} ions for seven days is shown in Fig. 13b and c. Fig. 13a shows an aggressive attack of the corroding medium on the steel surface. It further shows that the corrosion products appear very uneven and the surface layer is too rough. Fig. 13b and c reveals that SEM images of polished carbon steel immersed in the inhibitor solutions are in better conditions having smooth surface. This indicated that the inhibitor molecules hindered the dissolution of iron by forming protective film on the carbon steel surface and thereby reduced the rate of corrosion. Hence, the inhibitors protect carbon steel in control solution [17].

3.6. Mechanism of protection

A plausible mechanism of corrosion inhibition is proposed as follows,

Carbon steel undergoes initial corrosion to form Fe^{2+} ions at the anodic sites.



Fe^{2+} further undergoes oxidation in the presence of oxygen available in the aqueous solution.

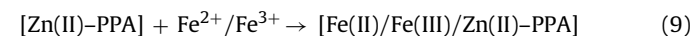


The corresponding reduction reaction at the cathodic sites in neutral and alkaline media is:



Fe^{3+} ions produced at anodic areas and OH^- ions produced at cathodic area combine to form $\text{Fe}(\text{OH})_3$. Apart from $\text{Fe}(\text{OH})_3$, there is formation of other oxides and hydroxides like FeOOH , $\gamma\text{-Fe}_2\text{O}_3$, etc., on the metal surface before the formation of protective film.

When, PPA and Zn^{2+} ions are added to the aqueous solution, PPA react with Zn^{2+} to form a $[\text{Zn}(\text{II})\text{-PPA}]$ complex. This complex diffuses to the metal surface and reacts with $\text{Fe}^{2+}/\text{Fe}^{3+}$ ions available at the anodic sites to form $[\text{Fe}(\text{II})/\text{Fe}(\text{III})/\text{Zn}(\text{II})\text{-PPA}]$ complex which covers the anodic sites and controls the corresponding reaction at anodic sites.



Free Zn^{2+} ions which are available in the bulk of the solution diffuse to the metal surface and react with OH^- ions produced at the

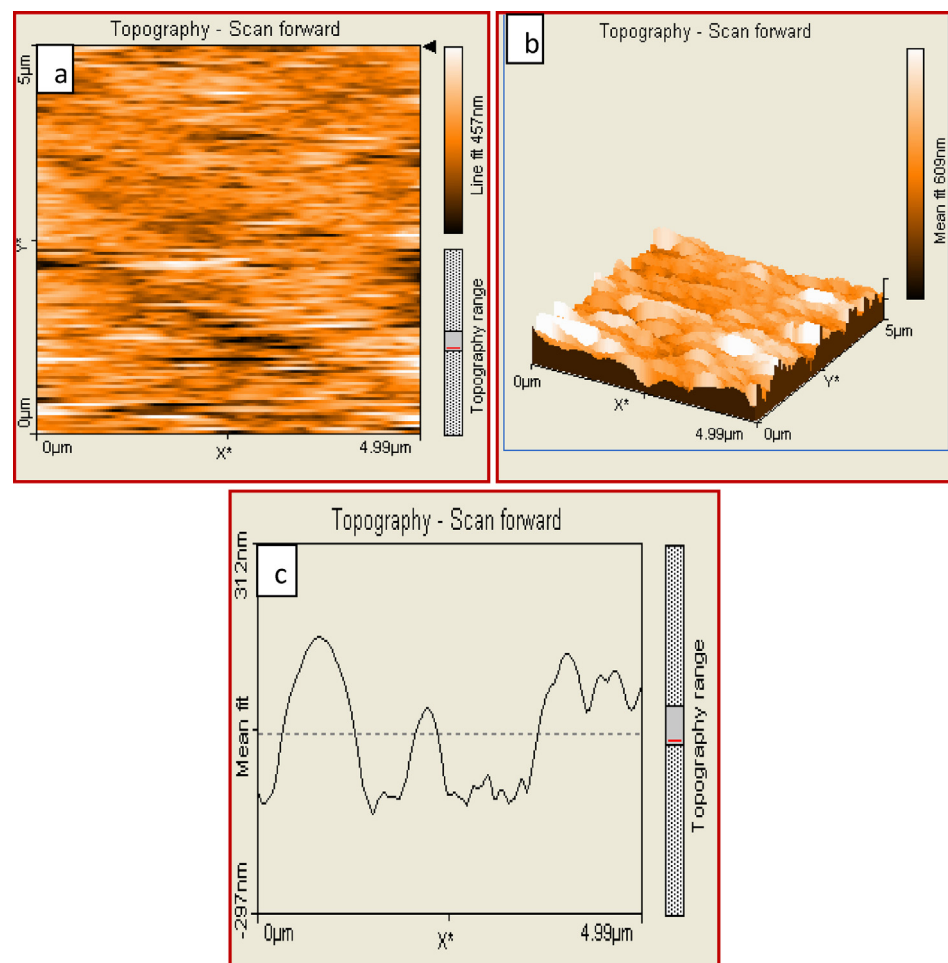


Fig. 12. AFM images and cross section analysis of polished metal surface immersed in 60 ppm Cl^- ion + 75 ppm PPA + 100 ppm Zn^{2+} ions.

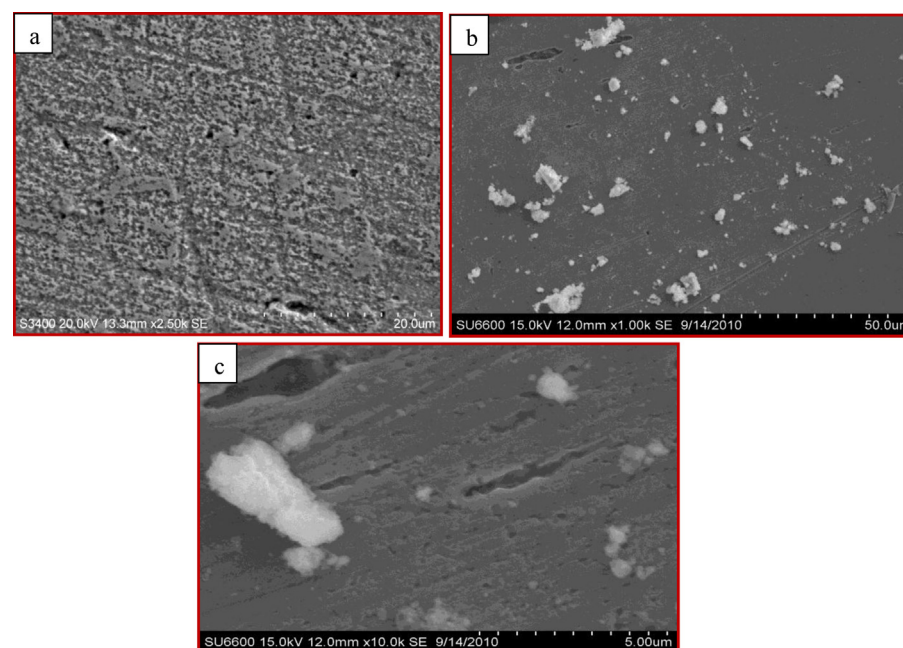


Fig. 13. SEM images of carbon steel immersed in (a) 60 ppm Cl^- , (b) and (c) 60 ppm Cl^- solution containing inhibitors 100 ppm Zn^{2+} + 75 ppm PPA.

cathodic sites to form a precipitate of $Zn(OH)_2$. This precipitate gets deposited on the cathodic sites and controls the cathodic reaction.



Thus, PPA and Zn^{2+} ions play a very important role in the synergistic effect in controlling corrosion through the formation of a protective film on the metal surface. Similar reports of complex formation have been observed in the literature [12,15,17].

4. Conclusion

- (1) Showed an excellent synergistic effect in the PPA-Zn²⁺ system.
- (2) The binary system 75 ppm PPA and 100 ppm Zn²⁺ is effective and has 90% IE.
- (3) The binary inhibitor system is effective in the pH range 6–8.
- (4) The inhibitor formulation acts as a mixed inhibitor predominantly cathodic in nature.
- (5) In presence of the inhibitor, the charge transfer resistance is significantly increased. The double layer capacitance of surface film is markedly decreased.
- (6) The protective film may consists of [Fe(III)/Fe(II)/Zn(II)-PPA] complex, $Zn(OH)_2$, hydroxides and oxides of iron.
- (7) This multi component formulation consisting of PPA and Zn²⁺ can be used as a potential inhibitor to prevent the corrosion of carbon steel in near neutral aqueous media.

Acknowledgements

One of the authors M. Prabakaran is grateful to the UGC for the fellowship under Research Fellowship in Sciences for Meritorious Students. The authors thank the Co-ordinator, UGC-SAP, Department of Chemistry, GRI for providing the support for recording XPS and also thank the authorities of Gandhigram Rural Institute for the encouragement.

References

- [1] M. Benabdellah, A. Dafali, B. Hammouti, A. Aouni, M. Rhomari, A. Raada, O. Senhaji, J.J. Robin, The role of phosphonate derivatives on the corrosion inhibition of steel in HCl media, *Chemical Engineering Communications* 194 (2007) 1328–1341.
- [2] D.J. Choi, S.J. You, J.G. Kim, Development of an environmentally safe corrosion, scale and microorganism inhibitor for open recirculating cooling systems, *Materials Science and Engineering: A* 335 (2002) 228–235.
- [3] H. Amar, J. Benzakour, A. Derja, D. Villemain, B. Moreau, T. Braisaz, Piperidin-1-yl-phosphonic acid and (4-phospho-piperazin-1-yl) phosphonic acid: a new class of iron corrosion inhibitors in sodium chloride 3% media, *Applied Surface Science* 252 (2006) 6162–6172.
- [4] T.A. Truc, N. Pebere, T.T.X. Hang, Y. Hervaud, B. Boutevin, Study of the synergistic effect observed for the corrosion protection of a carbon steel by an association of phosphates, *Corrosion Science* 44 (2002) 2055–2071.
- [5] G. Gunasekaran, R. Natarajan, N. Palaniswamy, The role of tartrate ions in the phosphonate based inhibitor system, *Corrosion Science* 43 (2001) 1615–1626.
- [6] S. Rajendran, B.V. Apparao, N. Palaniswamy, V. Periasamy, G. Karthikeyan, Corrosion inhibition by stainless complexes, *Corrosion Science* 43 (2001) 1345–1354.
- [7] S. Rajendran, B.V. Apparao, N. Palaniswamy, Synergistic and antagonistic effects existing among polyacrylamide, phenyl phosphonate and Zn²⁺ on the inhibition of corrosion of mild steel in a neutral aqueous environment, *Electrochimica Acta* 44 (1998) 533–537.
- [8] E. Kalman, Working party on corrosion inhibitors, EFC Publications, IOM Communications 11 (1994) 12.
- [9] Y. Gonzalez, M.C. Lafont, N. Pebere, F. Moran, Synergistic effect between zinc salt and phosphonic acid for corrosion inhibition of a carbon steel, *Journal of Applied Electrochemistry* 26 (1996) 1259–1265.
- [10] H. Amar, J. Benzakour, A. Derja, D. Villemain, B. Moreau, T. Braisaz, A. Tounsi, Synergistic corrosion inhibition study of Armco iron in sodium chloride by piperidin-1-yl-phosphonic acid-Zn²⁺ system, *Corrosion Science* 50 (2008) 124–130.
- [11] M. Prabakaran, S. Ramesh, V. Periasamy, Inhibitive properties of a phosphonate-based formulation for corrosion control of carbon steel, *Research on Chemical Intermediates* (2012), <http://dx.doi.org/10.1007/s11164-012-0858-5>.
- [12] I. Sekine, Y. Hirakawa, Effect of 1-hydroxyethylidene-1,1-diphosphonic acid on the corrosion of SS 41 steel in 0.3% sodium chloride solution, *Corrosion* 42 (1986) 272–277.
- [13] P. Poczik, I. Felioci, J. Telgadi, M. Kalaji, E. Kalman, Layer formation by 1,7-diphosphono-heptane, *Journal of the Serbian Chemical Society* 66 (2001) 859–870.
- [14] J.L. Fang, Y. Li, X.R. Ye, Z.W. Wang, Q. Liu, Passive films and corrosion protection due to phosphonic acid inhibitors, *Corrosion* 49 (1993) 266–271.
- [15] S. Rajendran, B.V. AppaRao, N. Palaniswamy, Investigation of the inhibiting effect of ethyl phosphonic acid-Zn²⁺ system, *Bulletin of Electrochemistry* 17 (2001) 171–174.
- [16] M.A. Pech-Canul, P. Bartolo-Perez, Inhibition effects of N-phosphono-methyl-glycine/Zn²⁺ mixtures on corrosion of steel in neutral chloride solutions, *Surface and Coatings Technology* 184 (2004) 133–140.
- [17] B.V. AppaRao, M. VenkateswaraRao, S. SrinivasaRao, B. Sreedhar, Tungstate as a synergist to phosphonate-based formulation for corrosion control of carbon steel in nearly neutral aqueous environment, *Journal of Chemical Sciences* 122 (2010) 639–649.
- [18] K. Juttner, Electrochemical impedance spectroscopy (EIS) of corrosion processes on inhomogeneous surfaces, *Electrochimica Acta* 35 (1990) 1501–1508.
- [19] T. Tsuru, S. Haruyama, B. Gijutsu, Corrosion monitor based on impedance method; construction and its application to homogeneous corrosion, *Journal of the Japanese Society of Corrosion Engineering* 27 (1978) 573–579.
- [20] G. Gunasekaran, L.R. Chauhan, Eco friendly inhibitor for corrosion inhibition of mild steel in phosphoric acid medium, *Electrochimica Acta* 49 (2004) 4387–4395.
- [21] M.S. Morad, An electrochemical study on the inhibiting action of some organic phosphonon compounds on the corrosion of mild steel in aerated acid solutions, *Corrosion Science* 42 (2000) 1307–1326.
- [22] A. Alagta, I. Felhosi, J. Teleghi, I. Bartotti, E. Kalman, Effect of metal ions on corrosion inhibition of pimeloyl-1,5-di-hydroxamic acid for steel in neutral solution, *Corrosion Science* 49 (2007) 2754–2766.
- [23] F. Mansfeld, M.W. Kendig, W.J. Lorenz, Corrosion inhibition in neutral aerated media, *Journal of the Electrochemical Society* 132 (1985) 290–296.
- [24] J. Ross Macdonald, Impedance spectroscopy and its use in analyzing the steady-state AC response of solid and liquid electrolytes, *Journal of Electroanalytical Chemistry* 223 (1987) 25–50.
- [25] K.F. Khaled, N. Hackerman, Ortho-substituted anilines to inhibit copper corrosion in aerated 0.5 M hydrochloric acid, *Electrochimica Acta* 49 (2004) 485–495.
- [26] C.T. Wang, S.H. Chen, H.Y. Ma, N.X. Wang, Study of the stability of self-assembled N-vinylcarbazole monolayers to protect copper against corrosion, *Journal of the Serbian Chemical Society* 67 (2002) 685–696.
- [27] F. Kadırgan, S. Suzer, Electrochemical and XPS studies of corrosion behaviour of a low carbon steel in the presence of FT2000 inhibitor, *Journal of Electron Spectroscopy and Related Phenomena* 114–116 (2001) 597–601.
- [28] R.D. Royd, J. Verron, K.E. Hall, C. Underhill, S. Hebbert, R. West, The cleanliness of stainless steel as determined by X-ray photoelectron spectroscopy, *Applied Surface Science* 17 (2001) 135–143.
- [29] N.T. Sugi, K. Nozawa, K. Aramaki, Ultrathin protective films prepared by modification of an N,N-dimethylalkylamine monolayer with chlorosilanes for preventing corrosion of iron, *Corrosion Science* 42 (2000) 1523–1538.
- [30] A. Welle, J.D. Liao, K. Kaiser, M. Grunze, U. Mäder, N. Blank, Interactions of N,N'-dimethylaminoethanol with steel surfaces in alkaline and chlorine containing solutions, *Applied Surface Science* 119 (1997) 185–198.
- [31] I. Felhosi, Zs. Keresztes, F.H. Karman, M. Mohai, I. Bertotti, E. Kalman, Effects of bivalent cations on corrosion inhibition of steel by 1-hydroxyethane-1,1-diphosphonic acid, *Journal of the Electrochemical Society* 146 (1999) 961–969.
- [32] F.H. Karman, I. Felhosi, E. Kalman, I. Cséry, L. Kovář, The role of oxide layer formation during corrosion inhibition of mild steel in neutral aqueous media, *Electrochimica Acta* 43 (1998) 69–75.
- [33] J.F. Moulder, W.F. Stickle, P.E. Sobol, K.D. Bamben, *Handbook of X-ray Photoelectron Spectroscopy: A Reference Book of Standard Spectra for Identification and Interpretation of XPS Data*, Physical Electronics, USA, 1995.
- [34] E. Kalman, F.H. Karman, I. Cséry, L. Kovář, J. Teleghi, D. Varga, The effect of calcium ions on the adsorption of phosphonic acid: a comparative investigation with emphasis on surface analytical methods, *Electrochimica Acta* 39 (1994) 1179–1182.
- [35] N.S. McIntyre, D.G. Zetaruk, X-ray photoelectron spectroscopic studies of iron oxides, *Analytical Chemistry* 49 (1977) 1521–1529.
- [36] S. Maroie, M. Savy, J.J. Verbist, ESCA and EPR studies of monomer, dimer and polymer iron phthalocyanines: involvements for the electrocatalysis of molecular oxygen reduction, *Inorganic Chemistry* 18 (1979) 2560–2567.
- [37] N. Ochoa, G. Baril, F. Moran, N. Pebere, Study of the properties of a multi-component inhibitor used for water treatment in cooling circuits, *Journal of Applied Electrochemistry* 32 (2002) 497–504.
- [38] M. Koudelka, J. Sanchez, J. Augustynski, On the nature of surface films formed on iron in aggressive and inhibiting polyphosphate solutions, *Journal of the Electrochemical Society* 129 (1982) 1186–1191.
- [39] N. Labjar, S.E.I. Hajjaji, M. Lebrini, M. Serghinidrissi, C. Jama, F. Bentiss, Enhanced corrosion resistance properties of carbon steel in hydrochloric acid medium by aminotris-(methyleneephosphonic): surface characterizations, *Journal of Materials and Environmental Science* 2 (4) (2011) 309–318.

- [40] G. Qinlin, C. Xianhua, Tribological behaviors of lanthanum-based phosphonate 3-aminopropyltriethoxysilane self-assembled films, *Applied Surface Science* 253 (2007) 6800–6806.
- [41] C. Viorney, Y. Chevrolot, D. Leonard, B.O. Aronsson, P. Pechy, H.J. Mathieu, P. Descouts, M. Gratzel, Surface modification of titanium with phosphonic acid to improve bone bonding: characterization by XPS and to F-SIMS, *Langmuir* 18 (2002) 2582–2589.
- [42] T. Keszthelyi, Z. Paszti, T. Rigo, O. Hakkel, J. Telegdi, L. Guczi, Investigation of solid surfaces modified by Langmuir–Blodgett monolayers using sum-frequency vibrational spectroscopy and X-ray photoelectron spectroscopy, *Journal of Physical Chemistry B* 110 (2006) 8701–8714.
- [43] P.K. Kar, Gurmeet Singh, Evaluation of nitrilotrimethylene phosphonic acid and nitrilotriacetic acid as corrosion inhibitors of mild steel in sea water, *ISRN Materials Science* (2011) 6, <http://dx.doi.org/10.5402/2011/167487> (article ID 167487).
- [44] W. Temesghen, P.M.A. Sherwood, Analytical utility of valence band X-ray photoelectron spectroscopy of iron and its oxides, with spectral interpretation by cluster and band structure calculations, *Analytical and Bioanalytical Chemistry* 373 (2002) 601–608.
- [45] K. Babic-Samardzija, K. Lupu, N. Hackerman, A.R. Barron Luttge, Inhibitive properties and surface morphology of a group of heterocyclic diazoles as inhibitors for acidic iron corrosion, *Langmuir* 21 (2005) 12187–12196.
- [46] K. Aramaki, Preparation of self-healing protective films on a zinc electrode treated in a cerium(III) nitrate solution and modified with sodium phosphate and cerium(III) nitrate, *Corrosion Science* 46 (2004) 1565–1579.
- [47] A. Paszternak, I. Felhosi, Z. Paszti, E. Kuzmann, A. Vertes, E. Kalman, L. Nyikos, Surface analytical characterization of passive iron surface modified by alkyl-phosphonic acid layers, *Electrochimica Acta* 55 (2010) 804–812.
- [48] D. De Filippo, A. Rossi, B. Elsener, S. Virtanen, XPS analytical characterization of amorphous alloys: Fe70Cr10P13C7, *Surface and Interface Analysis* 15 (1990) 668–674.
- [49] N.B. Colthup, L.H. Daly, S.E. Wiberley, *Introduction to Infrared and Raman Spectroscopy*, 3rd edn., Academic press, New York, 1990.
- [50] K. Nakamoto, *Infrared and Raman Spectra of Inorganic and Co-ordination Compounds*. Fourth Edition, Johnwiley& Sons, New York, 1986.
- [51] X.H. To, N. Pébère, N. Pelaprat, B. Boutevin, Y. Hervaud, A corrosion-protective film formed on a carbon steel by an organic phosphonate, *Corrosion Science* 39 (1997) 1925–1934.
- [52] N. Nakayama, Inhibitory effects of nitrilotris(methylenephosphonic acid) on cathodic reactions of steels in saturated Ca(OH)₂ solutions, *Corrosion Science* 42 (2000) 1897–1920.
- [53] K. Aramaki, Self-healing mechanism of a protective film prepared on a Ce(NO₃)₃-pretreated zinc electrode by modification with Zn(NO₃)₂ and Na₃PO₄, *Corrosion Science* 45 (2003) 1085–1101.
- [54] J. Li, D.J. Meier, An AFM study of the properties of passive films on iron surfaces, *Journal of Electroanalytical Chemistry* 454 (1998) 53–58.
- [55] B.D. Mert, M.E. Mert, G. Kardaş, B. Yazıcı, Experimental and theoretical studies on electrochemical synthesis of poly(3-amino-1,2,4-triazole), *Applied Surface Science* 258 (2012) 9668–9674.